電気学会論文誌●（●●●●●●●部門誌）
IEEJ Transactions on ●●●●●●●●●●●●●●●●
Vol.●● No.● pp.●-●● DOI: ●.●●/ieejeiss.●●.●

Paper

General Analytical Model of Inductance Variation with EMF-canceling Coil for Inductive Power Transfer System

Keita Furukawa*, Student member, Keisuke Kusaka*, Member,
Jun-ichi Itoh*a), Senior member

(Manuscript received Jan. 00, 20XX, revised May 00, 20XX)

This paper presents an analytical model and a design criteria for additional windings to reduce electromagnetic field (EMF) generated from inductive power transfer (IPT) systems. In particular, the canceling windings are connected to the main windings with common-mode connection, differential-mode connection, or short-circuited connection. Parameter variation, which may degrade the system efficiency, occurs in the IPT system owing to the unwanted coupling between the main windings and the canceling windings. Therefore, the theoretical analysis of the IPT system considering the canceling windings is conducted to evaluate the effects of the EMF shielding methods on system parameter variation. The calculation results of the system parameters agree with the measurement results in the prototype of the four-winding IPT coils, the error is lower than 5%. The simulation results with a 1-kW prototype IPT system indicate that the magnetic flux density at the distance of 50 cm from the bottom of the receiving coils decreases by at most 41% with the differential-mode connection.

Keywords : active shielding, electromagnetic field, inductive power transfer, multiple magnetic coupling

1. Introduction

In recent years, inductive power transfer (IPT) systems have attracted much attention in terms of safety and convenient battery chargers for electrical vehicles (EVs) [1–5]. The IPT systems achieve power transmission using a magnetic coupling without electrical contacts. Electromagnetic field (EMF) should be considered because EMF may cause health impairment or malfunction of electrical equipment [5–7]. In particular, high-power IPT systems such as quick battery chargers for EVs generate high level of EMF. Therefore, it is necessary to reduce radiation noise to widespread use of the IPT system.

In order to reduce EMF, many studies have been conducted on different circuit topologies, modulation methods and configurations of IPT coils [5–16]. In particular, non-resonant reactive shield and active shield, which are focused on the configurations of the IPT coils, have been proposed [11–14].

Non-resonant reactive shielding methods require additional short-circuited coils to reduce EMF [11–12]. The magnetic flux induces a current which cancels the leakage magnetic field in the short-circuited coils when a leakage magnetic flux crosses the short-circuited coils. However, the EMF-reduction effectiveness is low at the place far from the canceling windings because the magnetomotive force of the canceling winding is limited by the interlinkage magnetic flux [11].

On the other hand, the active shielding method employs canceling windings which are connected to the main windings or additional power sources [11–14]. In this method, the current flowing in the canceling windings is controllable with the main windings or the power sources. Therefore, the cancellation of the magnetic field becomes more effective compared to the non-resonant reactive shielding method because the magnetic field generated by the canceling windings are controllable [11].

The reduction effect of EMF by adding coils has been reported in several papers [11–16]. Nevertheless, parameter variations of the IPT coil due to the additional coils have not been analytically discussed. In particular, the magnetic flux generated by the canceling windings not only reduces the EMF but also crosses the main windings as an interlinkage flux. Thus, the self-inductance and the mutual inductance of the entire IPT coil change due to the additional coils [12]. This variation of the self-inductance changes the resonant frequency. Therefore, the transmission power or the efficiency might be affected compared that of the non-canceling windings. This problem in the past work is that the influences of adding the canceling windings to the entire IPT systems are not discussed in term of the inductance variation.

In this paper, the effect of the canceling windings is evaluated, focusing on the variations of the equivalent self-inductance and the equivalent mutual inductance of the entire IPT coil. In particular, a model of a four-winding IPT coils is theoretically analyzed. The contribution of this paper is to provide a general analytical model and design criteria to reduce the parameter variation due to the EMF canceling windings. In particular, the canceling windings are connected in parallel to the main windings to reduce EMF of IPT coils system as the non-resonant reactive shielding method or the active shielding method. The equivalent self-inductances and the equivalent coupling coefficient considering the influence of the canceling windings are calculated from a view of the entire transmission system. Then, the calculation results are confirmed with the measurement of the equivalent self-inductances and the equivalent coupling coefficient in prototypes of the four-winding IPT coils. Moreover, the effect of EMF reduction is simulated when the prototypes are installed to the 1-kW IPT systems.

a) Correspondence to: Jun-ichi Itoh. E-mail: itoh@vos.nagaokaut.ac.jp
* Nagaoka University of Technology.
1603-1, Kamitomioka-machi, Nagaoka, Niigata, Japan
940-2188

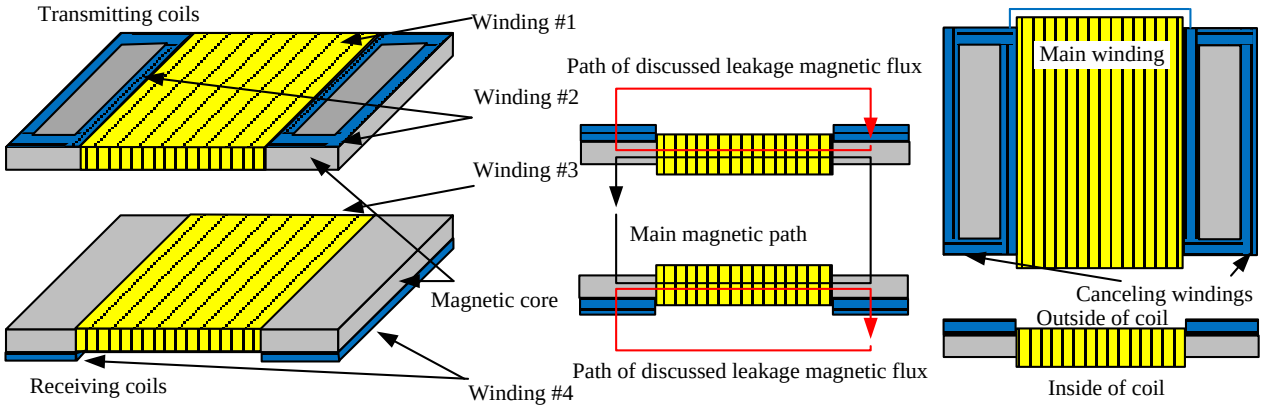

(a) Outline of transmission coil. (b) Front view with magnetic paths. (c) Configuration of coil at one side.

Fig. 1. Investigated model of IPT coil as example. The solenoid-type IPT coil with the canceling windings (winding #2 and winding #4). EMF upper and under cores is reduced by the canceling windings.

2. Configuration of IPT coils

Figure 1 shows the schematic of the analyzed IPT coils. Although following analysis is possible to be applied to general IPT coils, which fulfill some conditions as mentioned later, the solenoid-type IPT coil is analyzed as an example.

In general, canceling windings or conductive plates are installed around the circular pads in order to reduce EMF [11–15]. The conductive plates or the canceling windings cancel magnetic flux crossing themselves by the eddy current or the current of the coils [11–16]. Moreover, the eddy current or the current of the canceling windings generate antiphase magnetic field around the canceling windings or the conductive plates, which is useful to reduce leakage magnetic and EMF [11–16].

As shown in Fig. 1(b), the canceling windings are placed on the outside of the cores at the transmitting and receiving coils to reduce EMF which emits at the top and bottom the IPT coils. Both the transmitting coils and the receiving coils have same size and same configuration. The main windings, e.g. winding #1 and winding #3, are wired on the cores as typical solenoid coils. The canceling windings, e.g. winding #2 and winding #4, form a pair of the serial rectangular coil. The canceling windings are installed on the same core of the main windings. The four windings couples to each other magnetically. Therefore, the IPT coils behaves as the four-winding transformer.

Due to the placement of the canceling windings, the mutual inductances between following windings, e.g. winding #2 and winding #3, winding #2 and winding #4, and winding #4 and winding #1, are negligibly weak. Thus, the relationship among the current i_1, i_2, i_3, i_4 and the voltage v_1, v_2, v_3, v_4 of each windings in Fig. 1 is expressed by the four-order inductance matrix as

$$\begin{pmatrix} v_1 \\ v_2 \\ v_3 \\ v_4 \end{pmatrix} = L \begin{pmatrix} 1 & k_c\sqrt{\alpha} & k_M & 0 \\ k_c\sqrt{\alpha} & \alpha & 0 & 0 \\ k_M & 0 & 1 & k_c\sqrt{\alpha} \\ 0 & 0 & k_c\sqrt{\alpha} & \alpha \end{pmatrix} \frac{d}{dt} \begin{pmatrix} i_1 \\ i_2 \\ i_3 \\ i_4 \end{pmatrix} \quad \text{..... (1),}$$

where L is the self-inductance of the main windings, k_M and k_c are the coupling coefficients between the main winding and the main winding, and between the main winding and the canceling winding, respectively, and α is the self-inductance ratio between the main windings and the canceling windings.

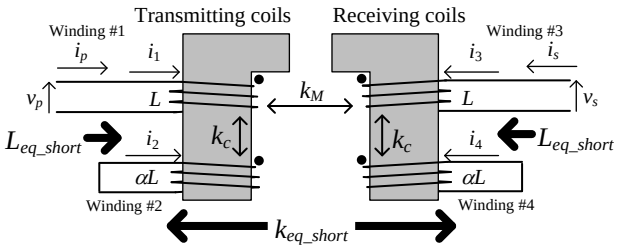

(a) Short-circuited canceling windings.

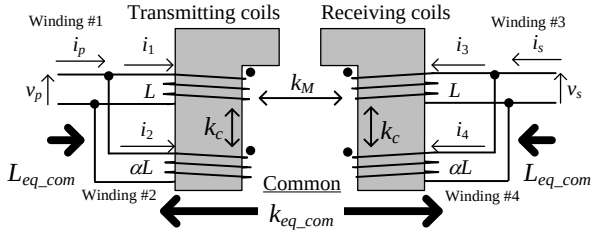

(b) Canceling windings connected as common-mode coils.

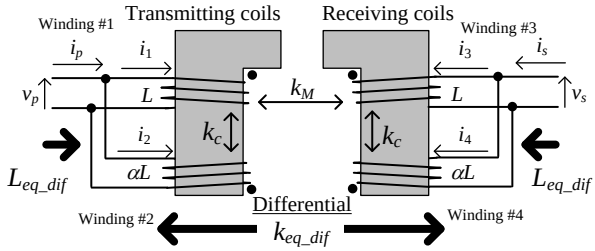

(c) Canceling windings connected as differential-mode coils.

Fig. 2. Connection diagrams of main windings and canceling windings.

Figure 2 shows the connection diagrams of the non-resonant reactive shielding method and the active shielding method. In the active shielding method, where the canceling windings are connected as the common-mode coils or the differential-mode coils, are considered. In particular, the common mode coils result in the positive mutual inductance between the parallel-connected coils, whereas the negative mutual inductance between the parallel-connected coils occurs in the differential mode coils.

3. Parameter Derivation

In this section, the equivalent self-inductance and the equivalent

coupling coefficient are formulated with a model of the multi-winding transformer when the canceling windings are connected to the main windings in parallel or short-circuited. The equivalent self-inductance is defined as self-inductances from the view of transmitting coils or receiving coils of the entire IPT coil. The equivalent coupling coefficient is defined as a coupling coefficient between the transmitting coils and the receiving coils. Both of the equivalent values are essential to design a resonant frequency and a transmission power for IPT systems.

3.1 Inverse Matrix of Inductance Matrix In order to clarify the equivalent self-inductance and the equivalent coupling coefficients, the inductance matrix is introduced in Eq. (1). It is convenient to calculate the current of the coils from the input voltage with the inverse matrix of the inductance matrix when conditions of the input voltage is decided as shown in Fig. 2. The relationship between the current and the voltage of each coil in Fig. 1 is also expressed by a four-order inverse matrix in (2), which is located at bottom of this page, and (3)

$$\det L = \alpha L\left\{\left(1+k_c\right)^2\left(1-k_c\right)^2 - {k_M}^2\right\} \quad \text{..... (3),}$$

where det L is the determinant of the four-order inductance matrix in (1).

3.2 Short-circuited Connection When the canceling windings are shorted as shown in Fig. 2(a), the input voltage is $v_1 = v_p$, $v_3 = v_s$ and $v_2 = v_4 = 0$. Hence, the input current is expressed by

$$\begin{pmatrix} i_1 \\ i_2 \\ i_3 \\ i_4 \end{pmatrix} = \frac{1}{\det L}\begin{pmatrix} \alpha\left(1-{k_c}^2\right) & -\alpha k_M \\ -\sqrt{\alpha}k_c\left(1-{k_c}^2\right) & \sqrt{\alpha}k_c k_M \\ -\alpha k_M & \alpha\left(1-{k_c}^2\right) \\ \sqrt{\alpha}k_c k_M & -\sqrt{\alpha}k_c\left(1-{k_c}^2\right) \end{pmatrix}\begin{pmatrix} \int v_p dt \\ \int v_s dt \end{pmatrix} \text{.. (4).}$$

In addition, the conditions of the input current $i_1 = i_p$, $i_3 = i_s$ are considered. The relationship between the voltage and the current of the entire IPT coils is shown as

$$\begin{pmatrix} i_p \\ i_s \end{pmatrix} = \begin{pmatrix} i_1 \\ i_3 \end{pmatrix} = \frac{\alpha}{\det L}\begin{pmatrix} 1-{k_c}^2 & -k_M \\ -k_M & 1-{k_c}^2 \end{pmatrix}\begin{pmatrix} \int v_p dt \\ \int v_s dt \end{pmatrix} \quad \text{..... (5),}$$

$$\begin{pmatrix} v_p \\ v_s \end{pmatrix} = \begin{pmatrix} L_{peq\_short} & M_{eq\_short} \\ M_{eq\_short} & L_{seq\_short} \end{pmatrix}\frac{d}{dt}\begin{pmatrix} i_p \\ i_s \end{pmatrix} = L\begin{pmatrix} 1-{k_c}^2 & k_M \\ k_M & 1-{k_c}^2 \end{pmatrix}\frac{d}{dt}\begin{pmatrix} i_p \\ i_s \end{pmatrix} \quad \text{..... (6),}$$

where L_{peq_short} is the equivalent self-inductance of the transmitting coils, L_{seq_short} is the equivalent self-inductance of the receiving coils, and M_{eq_short} is the equivalent mutual inductances between the transmitting coils and the receiving coils.

Then, the self-inductance and the coupling coefficient of the entire IPT coil are varied from the original values L and k_M, respectively due to the employment of the canceling windings. The equivalent self-inductance $L_{eq\text{-}short}$ (= L_{peq_short} = L_{seq_short}) and the equivalent coupling coefficient k_{eq_short} are expressed,

$$L_{eq\_short} = L\left(1-{k_c}^2\right) \quad \text{..... (7)}$$

$$k_{eq\_short} = \frac{M_{eq\_short}}{L_{eq\_short}} = \frac{k_M}{1-{k_c}^2} \quad \text{..... (8).}$$

3.3 Common-mode Connection The conditions of the input voltage is $v_1 = v_2 = v_p$ and $v_3 = v_4 = v_s$. Hence, when the canceling windings are connected to the main windings as the common-mode coils as shown in Fig. 2 (b), the input current is expressed by (9)

$$\begin{pmatrix} i_1 \\ i_2 \\ i_3 \\ i_4 \end{pmatrix} = \frac{1}{\det L}\begin{pmatrix} \sqrt{\alpha}\left(\sqrt{\alpha}-k_c\right)\left(1-{k_c}^2\right) & -\sqrt{\alpha}\left(\sqrt{\alpha}-k_c\right)k_M \\ \left(1-\sqrt{\alpha}k_c\right)\left(1-{k_c}^2\right)-{k_M}^2 & \left(\sqrt{\alpha}-k_c\right)k_c k_M \\ -\sqrt{\alpha}\left(\sqrt{\alpha}-k_c\right)k_M & \sqrt{\alpha}\left(\sqrt{\alpha}-k_c\right)\left(1-{k_c}^2\right) \\ \left(\sqrt{\alpha}-k_c\right)k_c k_M & \left(1-\sqrt{\alpha}k_c\right)\left(1-{k_c}^2\right)-{k_M}^2 \end{pmatrix}\begin{pmatrix} \int v_p dt \\ \int v_s dt \end{pmatrix} \quad \text{..... (9).}$$

In addition, the conditions of the input current $i_p = i_1 + i_2$, $i_s = i_3 + i_4$ are considered. The relationship between the voltage and the current of the entire IPT coils is shown in (10) and (11)

$$\begin{pmatrix} i_p \\ i_s \end{pmatrix} = \begin{pmatrix} i_1 + i_2 \\ i_3 + i_4 \end{pmatrix} = \frac{1}{\det L}\begin{pmatrix} \left(\alpha - 2\sqrt{\alpha}k_c + 1\right)\left(1-{k_c}^2\right)-{k_M}^2 & -\left(\sqrt{\alpha}-k_c\right)^2 k_M \\ -\left(\sqrt{\alpha}-k_c\right)^2 k_M & \left(\alpha - 2\sqrt{\alpha}k_c + 1\right)\left(1-{k_c}^2\right)-{k_M}^2 \end{pmatrix}\begin{pmatrix} \int v_p dt \\ \int v_s dt \end{pmatrix} \text{.. (10),}$$

$$\begin{pmatrix} v_p \\ v_s \end{pmatrix} = \begin{pmatrix} L_{peq\_com} & M_{eq\_com} \\ M_{eq\_com} & L_{seq\_com} \end{pmatrix}\frac{d}{dt}\begin{pmatrix} i_p \\ i_s \end{pmatrix} = \frac{\alpha L}{\left(\alpha - 2\sqrt{\alpha}k_c + 1\right)^2 - {k_M}^2}\begin{pmatrix} \left(\alpha - 2\sqrt{\alpha}k_c + 1\right)\left(1-{k_c}^2\right)-{k_M}^2 & \left(\sqrt{\alpha}-k_c\right)^2 k_M \\ \left(\sqrt{\alpha}-k_c\right)^2 k_M & \left(\alpha - 2\sqrt{\alpha}k_c + 1\right)\left(1-{k_c}^2\right)-{k_M}^2 \end{pmatrix}\frac{d}{dt}\begin{pmatrix} i_p \\ i_s \end{pmatrix} \quad \text{..... (11),}$$

where L_{peq_com} is the equivalent self-inductance of the transmitting coils, L_{seq_com} is the equivalent self-inductance of the receiving coils, and M_{eq_com} is the equivalent mutual inductances between

$$\begin{pmatrix} i_1 \\ i_2 \\ i_3 \\ i_4 \end{pmatrix} = L^{-1}\begin{pmatrix} 1 & k_c\sqrt{\alpha} & k_M & 0 \\ k_c\sqrt{\alpha} & \alpha & 0 & 0 \\ k_M & 0 & 1 & k_c\sqrt{\alpha} \\ 0 & 0 & k_c\sqrt{\alpha} & \alpha \end{pmatrix}^{-1}\begin{pmatrix} \int v_1 dt \\ \int v_2 dt \\ \int v_3 dt \\ \int v_4 dt \end{pmatrix} = \frac{1}{\det L}\begin{pmatrix} \alpha\left(1-{k_c}^2\right) & -\sqrt{\alpha}k_c\left(1-{k_c}^2\right) & -\alpha k_M & \sqrt{\alpha}k_c k_M \\ -\sqrt{\alpha}k_c\left(1-{k_c}^2\right) & \left(1-{k_c}^2\right)-{k_M}^2 & \sqrt{\alpha}k_c k_M & -{k_c}^2 k_M \\ -\alpha k_M & \sqrt{\alpha}k_c k_M & \alpha\left(1-{k_c}^2\right) & -\sqrt{\alpha}k_c\left(1-{k_c}^2\right) \\ \sqrt{\alpha}k_c k_M & -{k_c}^2 k_M & -\sqrt{\alpha}k_c\left(1-{k_c}^2\right) & \left(1-{k_c}^2\right)-{k_M}^2 \end{pmatrix}\begin{pmatrix} \int v_1 dt \\ \int v_2 dt \\ \int v_3 dt \\ \int v_4 dt \end{pmatrix} \quad \text{..... (2)}$$

the transmitting coils and the receiving coils. The equivalent self-inductance L_{eq_com} (= L_{peq_com} = L_{seq_com}) and the equivalent coupling coefficient k_{eq_com} are expressed in (12) and (13)

$$L_{eq\_com} = \frac{\alpha L\left\{\left(1-k_c{}^2\right)\left(1+\alpha-2k_c\sqrt{\alpha}\right)-k_M{}^2\right\}}{\left(\alpha-2\sqrt{\alpha}k_c+1\right)^2-k_M{}^2} \quad \text{..... (12)}$$

$$k_{eq\_com} = \frac{M_{eq\_com}}{L_{eq\_com}} = \frac{k_M\left(\sqrt{\alpha}-k_c\right)^2}{\left(1-k_c{}^2\right)\left(1+\alpha-2k_c\sqrt{\alpha}\right)-k_M{}^2} \quad \text{..... (13).}$$

3.4 Differential-mode Connection The conditions of the input voltage is $v_1 = -v_2 = v_p$ and $v_3 = -v_4 = v_s$ when the canceling windings are connected to the main windings as the differential-mode coils as shown in Fig. 2 (c). Hence, the input current is expressed by (14)

$$\begin{pmatrix} i_1 \\ i_2 \\ i_3 \\ i_4 \end{pmatrix} = \frac{1}{\det L}\begin{pmatrix} \sqrt{\alpha}\left(\sqrt{\alpha}+k_c\right)\left(1-k_c{}^2\right) \\ \left(1+\sqrt{\alpha}k_c\right)\left(1-k_c{}^2\right)-k_M{}^2 \\ -\sqrt{\alpha}\left(\sqrt{\alpha}+k_c\right)k_M \\ \left(\sqrt{\alpha}+k_c\right)k_ck_M \end{pmatrix}$$

$$\begin{pmatrix} -\sqrt{\alpha}\left(\sqrt{\alpha}+k_c\right)k_M \\ \left(\sqrt{\alpha}+k_c\right)k_ck_M \\ \sqrt{\alpha}\left(\sqrt{\alpha}+k_c\right)\left(1-k_c{}^2\right) \\ \left(1+\sqrt{\alpha}k_c\right)\left(1-k_c{}^2\right)-k_M{}^2 \end{pmatrix}\begin{pmatrix} \int v_p dt \\ \int v_s dt \end{pmatrix} \quad \text{..... (14).}$$

In addition, the conditions on the input current $i_p = i_1 - i_2$, $i_s = i_3 - i_4$ are considered. The relationship between the voltage and the current of the entire IPT coils is shown in (15) and (16)

$$\begin{pmatrix} i_p \\ i_s \end{pmatrix} = \begin{pmatrix} i_1-i_2 \\ i_3-i_4 \end{pmatrix} = \frac{1}{\det L}\begin{pmatrix} \left(\alpha+2\sqrt{\alpha}k_c+1\right)\left(1-k_c{}^2\right)-k_M{}^2 \\ -\left(\sqrt{\alpha}+k_c\right)^2k_M \end{pmatrix}$$

$$\begin{pmatrix} -\left(\sqrt{\alpha}+k_c\right)^2k_M \\ \left(\alpha+2\sqrt{\alpha}k_c+1\right)\left(1-k_c{}^2\right)-k_M{}^2 \end{pmatrix}\begin{pmatrix} \int v_p dt \\ \int v_s dt \end{pmatrix} \text{. (15),}$$

$$\begin{pmatrix} v_p \\ v_s \end{pmatrix} = \begin{pmatrix} L_{peq\_dif} & M_{eq\_dif} \\ M_{eq\_dif} & L_{seq\_dif} \end{pmatrix}\frac{d}{dt}\begin{pmatrix} i_p \\ i_s \end{pmatrix}$$

$$= \frac{\alpha L}{\left(\alpha+2\sqrt{\alpha}k_c+1\right)^2-k_M{}^2}\begin{pmatrix} \left(\alpha+2\sqrt{\alpha}k_c+1\right)\left(1-k_c{}^2\right)-k_M{}^2 \\ \left(\sqrt{\alpha}+k_c\right)^2k_M \end{pmatrix}$$

$$\begin{pmatrix} \left(\sqrt{\alpha}+k_c\right)^2k_M \\ \left(\alpha+2\sqrt{\alpha}k_c+1\right)\left(1-k_c{}^2\right)-k_M{}^2 \end{pmatrix}\frac{d}{dt}\begin{pmatrix} i_p \\ i_s \end{pmatrix} \quad \text{.....(16),}$$

where L_{peq_dif} is the equivalent self-inductance of the transmitting coils, L_{seq_dif} is the equivalent self-inductance of the receiving coils, and M_{eq_dif} is the equivalent mutual inductances between the transmitting coils and the receiving coils. The equivalent self-inductance L_{eq_dif} (= L_{peq_dif} = L_{seq_dif}) and the equivalent coupling coefficient k_{eq_dif} are expressed in (17) and (18)

$$L_{eq\_dif} = \frac{\alpha L\left\{\left(1-k_c{}^2\right)\left(1+\alpha+2k_c\sqrt{\alpha}\right)-k_M{}^2\right\}}{\left(\alpha+2\sqrt{\alpha}k_c+1\right)^2-k_M{}^2} \quad \text{..... (17)}$$

$$k_{eq\_dif} = \frac{M_{eq\_dif}}{L_{eq\_dif}} = \frac{k_M\left(\sqrt{\alpha}+k_c\right)^2}{\left(1-k_c{}^2\right)\left(1+\alpha+2k_c\sqrt{\alpha}\right)-k_M{}^2} \quad \text{.....(18).}$$

3.5 Design Criteria of Canceling Windings Figure 3 and 4 show the contour diagrams of the equivalent coupling coefficients and the equivalent self-inductances derived from Eqs. (7–8, 12–13, 17–18), respectively. Noted that the coupling coefficient k_M is fixed at 0.2, whereas the coupling coefficient k_c and the self-inductance ratio α are variables. In particular, k_c is adjusted by changing installation location and configuration of the canceling windings, whereas α is also adjusted by changing the number of the turns of the canceling windings.

Figure 3(a) shows that k_{eq_short} is improved by increasing k_c, whereas k_{eq_short} is not varied by α. Meanwhile, Fig. 4(a) shows that the L_{eq_short} is decreased by increase k_c, and L_{eq_short} is also not varied by α. Hence, the parameter variation with the short-circuited canceling windings is not influenced by the number of the turns of the canceling windings.

Figure 3(b) shows that k_{eq_com} is improved by increasing k_c or α. Figure 4(b) shows that L_{eq_com} is decreasing due to the increase in k_c or the decrease in α. Thus, in order to avoid the parameter variation which is caused by the common-mode-connected canceling windings, not only the number of the turns of the canceling windings should be designed larger than the number of the turns of the main windings, but also the canceling windings have to be placed close to the main windings.

Figure 3(c) shows that k_{eq_dif} is improved in the range of high k_c and high α. Meanwhile, Fig. 4(c) shows that L_{eq_dif} is decreasing due to the high k_c and the decrease in α. Therefore, not only the winding turn should be much larger than the main windings, but also the canceling windings have to be installed apart from the main winding in order to avoid the parameter variation which is caused by the differential-mode-connected canceling windings.

However, setting the canceling windings apart from the main windings degrades a canceling performance of EMF. There is the trade-off between the parameter variation (decreasing of the equivalent self-inductance) and the canceling performance. Thus, an operation frequency or the construction of an IPT coil should be redesigned, when the canceling windings are installed in order to reduce EMF.

In addition, the weight and the volume increases for the canceling windings. The IPT coils with the common mode or the differential mode are heavier than the IPT coils with the short-circuited connection to avoid the decrease of the equivalent self-inductance. The turn number of the canceling windings with the common mode and the differential mode needs to be much larger because L_{eq_com} and L_{eq_dif} are decreased by low aL. Meanwhile, the turn number of the canceling windings with the short-circuited can be low because L_{eq_short} is not related to the number of the turn of the canceling windings.

As a conclusion, it is shown that the design criteria for the three connection methods of the canceling windings at the view point of avoiding the parameter variations as follows:

1) the short-circuited connection (non-resonant reactive shield)

- the long distance between the main windings and the

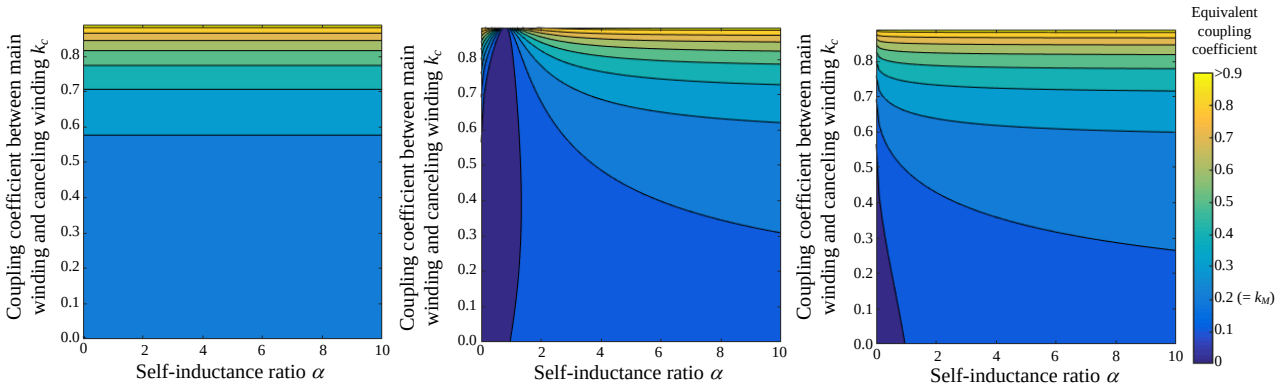

(a) k_{eq_short} (Short-circuited connection). (b) k_{eq_com} (Common mode). (c) k_{eq_dif} (Differential mode).

Fig. 3. Relationship among equivalent coupling coefficients, coupling coefficient between main winding and canceling winding, and self-inductance ratio. The coupling coefficient k_M is 0.2. Variation range of the coupling coefficient between the main winding and the canceling winding k_c is from 0 to 0.89, whereas range of the self-inductance ratio α is from 0 to 10.

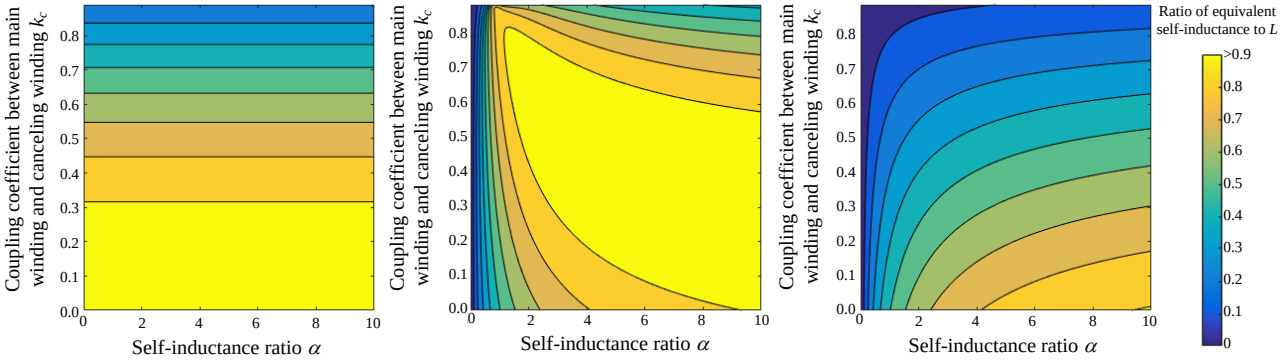

(a) L_{eq_short} / L (Short-circuited connection). (b) L_{eq_com} / L (Common mode). (c) L_{eq_dif} / L (Differential mode).

Fig. 4. Relationship among ratio of equivalent self-inductances to self-inductance of main windings, coupling coefficient between main windings and canceling windings, and self-inductance ratio. Conditions of k_M, k_c, and α are same as in Fig. 3.

canceling windings.

- the low self-inductance of the canceling windings.

2) the common-mode connection

- installation of the canceling windings by the main windings.
- twice or more the number of the turn of the canceling windings compared with the main windings.

3) the differential-mode connection

- the long distance between the main windings and the canceling windings.
- twice or more the number of the turn of the canceling windings compared with the main windings.

The advantage of avoiding the parameter variations is reducing the mismatch between the operation frequency and the resonant frequency, which is necessary to operate IPT systems under the conditions of the high efficiency and the high power transmission.

4. Experimental Verification with Prototype of IPT coil

The self-inductances and the mutual inductances of the wired coils are measured in order to confirm Eqs. (7–8, 12–13, 17–18) with the prototype four-winding IPT coil.

Figure 5 shows the prototype of the IPT coil. In order to shield EMF on the top and below, the canceling windings shaped double-D are put on the outside cores. The core material is ferrite (TDK Corp., N87). The number of turns of the main windings is 30 with 3.5-mm^2 insulated wires, whereas the number of turn of the canceling windings is 130 with enameled wires. Note that the number of turns of the transmitting coils and the receiving coils are the same.

Table I shows the measurement results of the four-order inductance matrix, the equivalent self-inductances and the equivalent coupling coefficients in the each connection. In order to compare the equivalent self-inductance, the equivalent mutual inductance, and the equivalent coupling coefficient, both the measured values and the calculated values are shown. The parameters of L, α and k_c are average values of the transmitting coils and the receiving coils. Note that the self-inductance, the mutual inductance and the equivalent coupling coefficient without the canceling windings are equal to L, k_ML and k_M, respectively, because the open coils do not influence the magnetic field.

In particular, the calculated values of the equivalent self-inductances correspond to the measured values with a maximum error of 2.7%. The self-inductance is the important factor because the IPT system should be designed to resonate at the transmission frequency. Thus, a precise calculation is crucial for the design of the IPT system. Besides, the maximum error of the equivalent coupling coefficients is 4.9%, which is larger than the error of the equivalent self-inductance because of the influence of the ignored magnetic coupling between following windings, i.e.,

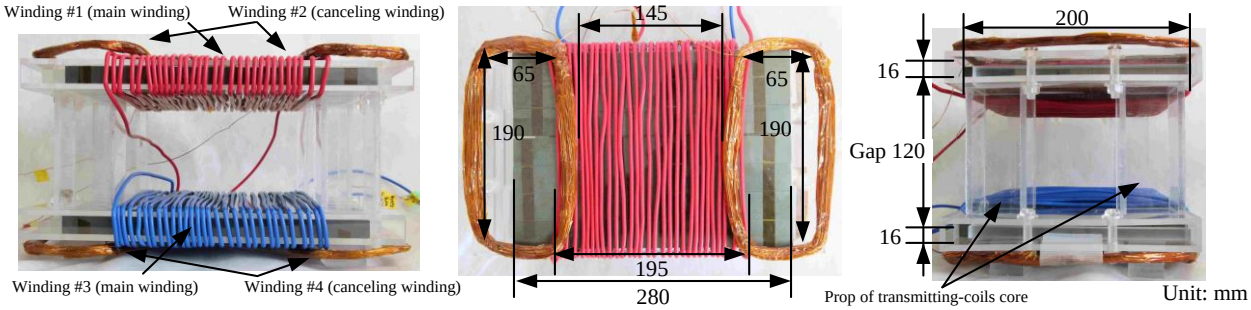

(a) Front view. (b) Top view. (c) Side view.

Fig. 5. Outline of prototype of four-winding IPT coils. The main windings are wired on center of the cores (winding #1 and winding #3). The canceling windings are put on top of the transmitting-coils core and bottom of the receiving-coils core (winding #2 and winding #4). The canceling windings construct the serial two coils. The four props support the transmitting-coils core.

Table I. Experimental results: equivalent coupling coefficient and inductances of prototype of four-winding IPT coils.

Connection of canceling windings		W/o canceling windings	Short-circuited	Common mode	Differential mode
Inductance matrix as four-winding IPT coils		$\begin{pmatrix} 399 & 432 & 70.4 & 12.2 \\ 432 & 3120 & 12.8 & 6.7 \\ 70.4 & 12.8 & 393 & 422 \\ 12.2 & 6.7 & 422 & 3010 \end{pmatrix}$ [μH]			
Self-inductance of main winding L	Average value	396 μH			
Self-inductance ratio α	Average value	7.94			
Coupling coefficient k_c	Average value	0.382			
Coupling coefficient k_M	Measured value	0.178			
Equivalent transmitting self-inductance	Measured value	399 μH	334 μH	396 μH	236 μH
	Calculated value		338 μH	394 μH	241 μH
Error of calculated equivalent transmitting self-inductance			1.3%	0.6%	2.3%
Equivalent receiving self-inductance	Measured value	393 μH	332 μH	391 μH	235 μH
	Calculated value		338 μH	394 μH	241 μH
Error of calculated equivalent receiving self-inductance			1.9%	0.7%	2.7%
Equivalent mutual inductance	Measured value	70.4 μH	67.5 μH	73.0 μH	43.3 μH
	Calculated value		70.4 μH	72.1 μH	46.6 μH
Equivalent coupling coefficient	Measured value	0.178	0.203	0.185	0.184
	Calculated value		0.208	0.183	0.193
Error of calculated coupling coefficient			2.7%	1.2%	4.9%

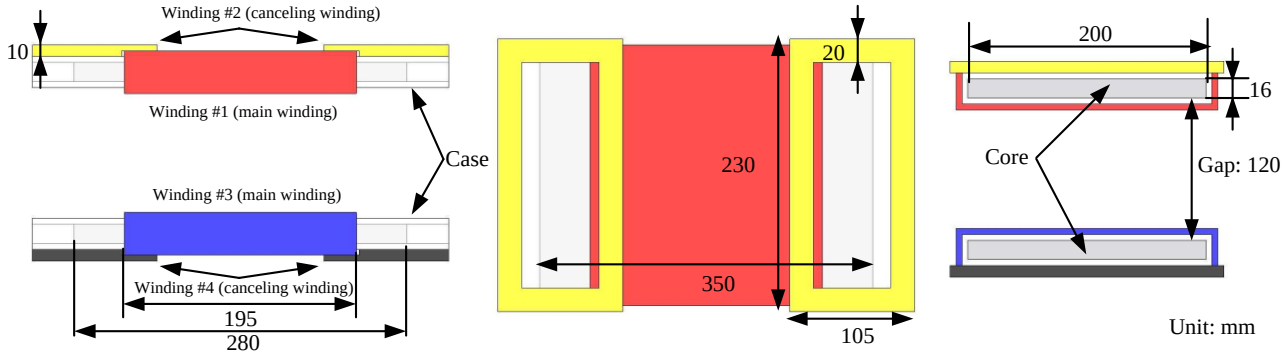

(a) Front view. (b) Top view. (c) Side view.

Fig. 6. Outline of CAD model of prototype four-winding IPT coils. The size of the cores and the cases matches the prototype of the four-winding IPT coils; the windings are constructed as the solid model, and the material of the cores is PC40. The cases are treated as air, whereas the thickness of the cases and the main windings is 5 mm.

winding #2 to winding #3, winding #2 to winding #4, and winding #4 to winding #1.

5. EMF Reduction with Canceling Windings

5.1 Circuit and Model Configuration

In this chapter, the IPT coils are simulated with JMAG (JSOL Corporation) to confirm the EMF reduction of the IPT coils with the canceling windings. JMAG is a software for the electromagnetic field analysis with a finite element method. The following electromagnetic field analysis is considered with only IPT coils at the fundamental harmonics component for simplification because the magnetic flux distribution around the IPT coils depends on the waveforms of the power source, forms and materials of EVs. Thus, the following measuring methods do not follow the guidelines such as ICNRP 2010. Note that the conventional method is considered as the two-winding IPT coils without the canceling windings.

Figure 6 shows the computer-aided-design (CAD) model of the

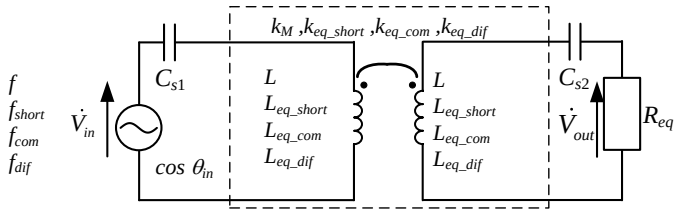

Fig. 7. Circuit configuration of simulation model. The prototype of the four-winding IPT coils is equivalent to the two-winding IPT coils when the canceling windings are shorted or connected to the main windings in parallel. For individual connection such as when the canceling windings are shorted, the equivalent self-inductance, the equivalent coupling coefficient and the operation frequency are chosen L_{eq_short}, k_{eq_short} and f_{short} differently.

IPT coil on JMAG. The structure and the size of the CAD model are based on the prototype of the four-winding IPT coil as shown in Fig. 5. The wires are expressed as the colored solid models. Noted that the eddy current and hysteresis loss are not considered.

Figure 7 shows the circuit configuration in the simulation model, whereas Table II shows the specification of the circuit. The IPT system is constructed with S/S topology, which has the resonant capacitors connected to both of the transmitting coils and the receiving coils of the IPT coil in series. The input voltage is the sinusoidal wave for focusing on fundamental frequency. The capacitances of the resonant capacitors C_{s1}, C_{s2} are decided in order to resonate with the considered L at a resonance frequency of 84.75 kHz. Noted that operating frequency is decided by the resonant conditions of the resonance capacitances and the equivalent self-inductance such as L_{eq_short}, L_{eq_com}, or L_{eq_dif}. The output power is 1 kW by adjusting the value of the equivalent load resistance R_{eq} because the output current of the S/S resonant circuit is inversely proportional to the equivalent mutual inductance of the IPT coil at the LC resonance.

5.2 EMF Reduction Effect with Canceling Windings Figure 8 shows the simulation results of the magnetic flux distribution under the each condition. The result is obtained on the cross-section of the center of the IPT coil as a representative case. Note that the input power factor $\cos\theta_{in}$ is unity when the operation frequencies of Fig. 8(a)–(d) are 84.75 kHz, 95.00 kHz, 85.40 kHz, 115.5 kHz, respectively.

The flux distributions on the top and bottom of the IPT coils decreases with the short-circuited connection and differential-mode connection in comparison with the flux distribution without the canceling windings. The magnetic flux distribution of Fig. 8(a)–(d) are 13.8 μT, 9.41 μT, 12.6 μT, and 8.06 μT at the 50-cm bottom of the receiving coils as the representative values, respectively. In addition, the magnetic density at the outside of the canceling winding decreases by the canceling windings. Moreover, the effect of EMF reduction is more effective with the differential mode than that with the short-circuited connection.

5.3 Current of Each Winding Figure 9 shows the RMS values of the current in each winding. The current of the canceling windings increases with the connection of the common mode, the short-circuited and the differential mode. The relation of the RMS values of the current in the canceling windings are similar to the EMF reduction effect in Fig. 8. On the other hand, the RMS values of the output voltage V_{out} are 165 V, 200 V, 183 V and 160 V without the canceling coils, with the short-circuited connection, the common-mode connection and the differential-mode connection, respectively, which are not shown large differences. Thus, the RMS current value of the canceling windings, which effects the system efficiency, forms the trade-off relationship with the EMF reduction effectiveness.

Table II. Simulation conditions.

Parameter	Symbol	Value
Input AC voltage	V_{in}	252 Vrms
Rated power	P	1.0 kW
Operation frequency without canceling windings	f	84.75 kHz
Operation frequency with short-circuited connection	f_{short}	95.00 kHz
Operation frequency with common-mode connection	f_{com}	85.40 kHz
Operation frequency with differential-mode connection	f_{dif}	115.5 kHz
Resonant capacitors	C_{s1} ,C_{s2}	8.56 nF

Figure 10 shows the estimate of the copper losses in the each winding from the RMS values of the current in the main windings and the canceling winding in Fig. 9. The equivalent serial resistances of each winding are measured with the prototype of the four-winding IPT coils in Fig. 5. The values of equivalent serial resistances from the winding #1 to the winding #4 are 1.39 Ω, 35.5 Ω, 1.57 Ω and 34.6 Ω, respectively. The total estimated copper loss becomes higher in the ascendant order: the w/o-canceling windings, the common-mode connection, the short-circuited connection and the differential-mode connection. In particular, the values of the copper losses on the canceling windings with the short-circuited connection and the differential-mode connection are not negligible at a view of the efficiency of the whole IPT coils.

6. Conclusion

In this paper, the effect of the canceling windings on the parameter variation of the IPT system was considered regarding to the equivalent self-inductance and the equivalent coupling coefficient. Three connection methods of the canceling windings, i.e. the short-circuited connection, the common-mode connection and the differential-mode connection, were evaluated.

The calculated equivalent values agreed with the measured values through the inductance measurement using the prototype of the IPT coil attached the canceling windings. The relative error between the calculated values and measured values was 4.9%.

In addition, EMF reduction near the canceling windings were confirmed with the short-circuit connection (by 32%) and the differential-mode connection (by 41%) in the simulation using JMAG.

Above of the results, the design criteria focusing on avoiding

the parameter verifications are as follows:

- the canceling windings far from the main windings at the short-circuited connection.
- the canceling windings closed to the main windings with the large number of the turn at the common-mode connection.
- the canceling windings far from the main windings with the large number of the turn at the differential-mode connection.

Future plans are considerations of the parameter verifications introduced cross couplings between canceling windings.

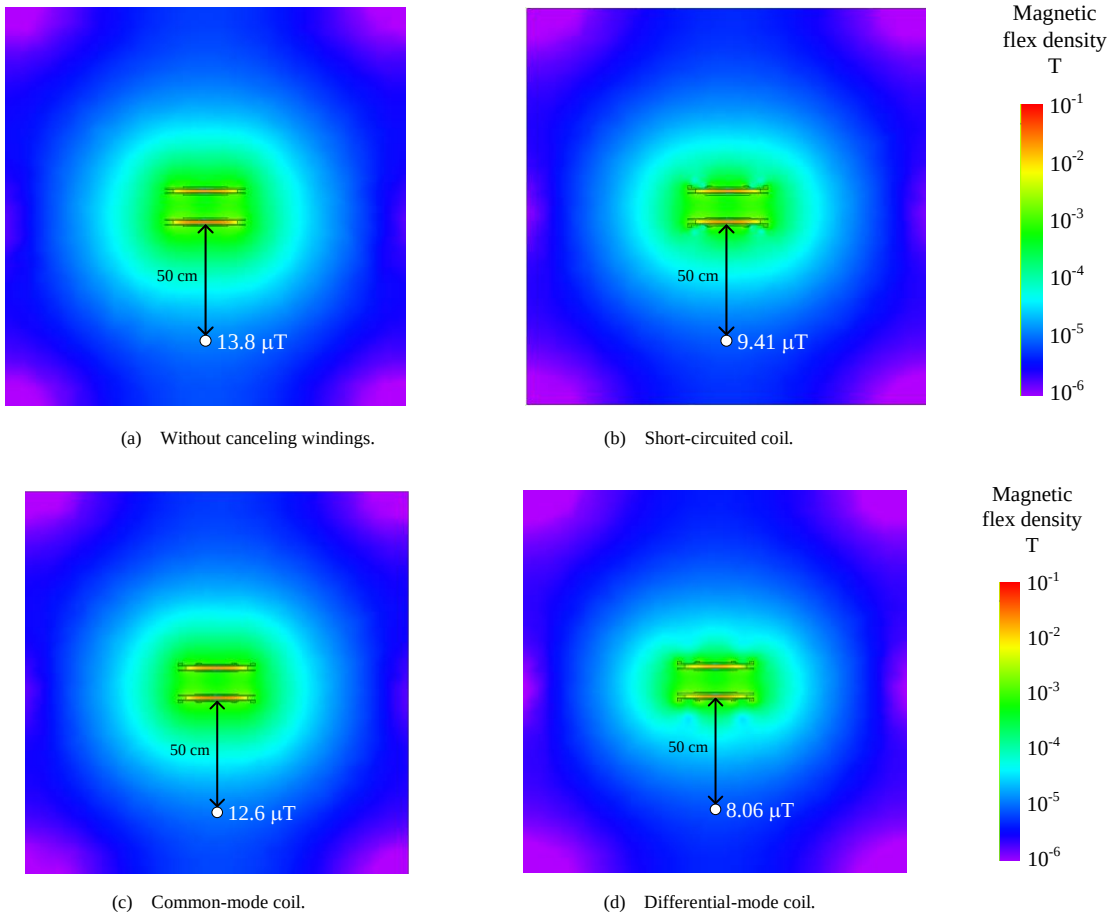

(a) Without canceling windings. (b) Short-circuited coil.

(c) Common-mode coil. (d) Differential-mode coil.

Fig. 8. Magnetic flux distribution of prototype transmission coil. The transmission coils are placed at the center of the contour plots (orange or yellow area). The upper-side core is the transmitting coils. The bottom-side core is the receiving coils. Note that the operation frequency is different for each the simulation conditions, which are shown in Table II. Transmission powers of without-canceling windings, short-circuited connection, common-mode connection and differential-mode connection are 991 W, 1.16 kW, 1.03 kW and 1.27 kW, respectively.

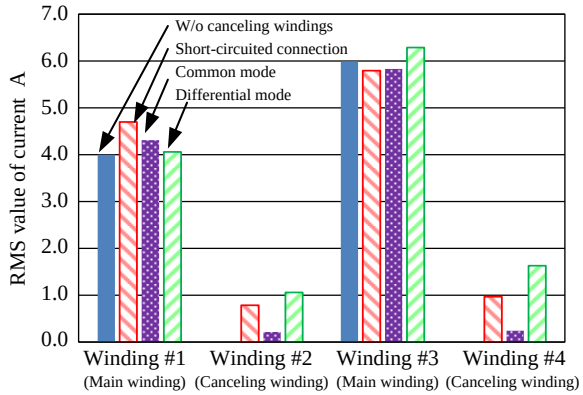

Fig. 9. RMS values of current. The blue, red, violet and green bars indicate the RMS value of the current w/o the canceling windings, the short-circuited, the common mode and the differential mode, respectively.

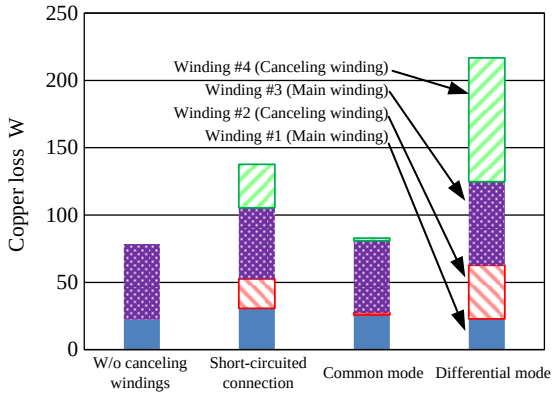

Fig. 10. Estimate of copper loss in each winding. The blue, red, violet and green bars indicate the copper loss from the winding #1 to the winding #4, respectively.

References

(1) T. Mizuno, T. Ueda, S. Yachi, R. Ohtomo and Y. Goto: "Dependence of Efficiency on Wire Type and Number of Strands of Litz Wire for Wireless Power Transfer of Magnetic Resonant Coupling", IEEJ Journal of Industry Applications, Vol. 3, No. 1, pp. 35-40 (2014)

(2) H. Ishida, H. Furukawa and T. Kyoden: "Development of Design Methodology for 60 Hz Wireless Power Transmission System", IEEJ Journal of Industry Applications, Vol. 5, No. 6, pp. 429-438 (2016)

(3) K. Kusaka, and J. Itoh: "Development Trends of Inductive Power Transfer Systems Utilizing Electromagnetic Induction with Focus on Transmission Frequency and Transmission Power", IEEJ Journal of Industry Applications, Vol. 137, No. 5, pp. 328-339 (2017)

(4) R. Ota, N. Hoshi and J. Haruna: "Design of Compensation Capacitor in S/P Topology of Inductive Power Transfer System with Buck or Boost Converter on Secondary Side", IEEJ Journal of Industry Applications, Vol. 4, No. 4, pp. 476-485 (2015)

(5) Su Y. Choi, Beom W. Gu, Seog Y. Jeong and Chun T. Rim: "Advances in Wireless Power Transfer Systems for Roadway-Powered Electric Vehicles", IEEE TRANSACTIONS ON POWER ELECTRONICS, Vol.3, No.1 pp.18 - 36 (2015)

(6) D. Shimode, T. Murai and S. Fujiwara: "A Study of Structure of Inductive Power Transfer Coil for Railway Vehicles", IEEJ Journal of Industry Applications, Vol. 4, No. 5, pp. 550-558 (2015)

(7) T. Watanabe and M. Ishida: "Study on the influence of the magnetic field and the induced electrical field in human bodies by wireless charging systems", EVTec and APE 2016, (2016)

(8) K. Kusaka, K. Inoue and J. Itoh: "Radiation Noise Reduction using Spread Spectrum for Inductive Power Transfer Systems considering Misalignment of Coils", Energy Conversion Congress and Exposition, pp. 5507-5514 (2017)

(9) T. Shijo, K. Ogawa, M. Suzuki, Y. Kanekiyo and M. Ishida: "EMI Reduction Technology in 85 kHz Band 44 kW Wireless Power Transfer System for Rapid Contactless Charging of Electric Bus", IEEE Energy Conversion Congress and Exposition (2016)

(10) T. Campi and Silvano Cruciani Mauro Feliziani: "Magnetic Shielding of Wireless Power Transfer Systems", Institute of Electronics, Information and Communication Engineers, 15A-H1, pp. 422-425 (2014)

(11) J. Park, D. Kim, K. Hwang, H. Ho Park and S. Il Kwak: "A Resonant Reactive Shielding for Planar Wireless Power Transfer System in Smartphone Application", IEEE TRANSACTIONS ON ELECTROMAGNETIC COMPATIBILITY, Vol. 59, No. 2, pp. 695-703 (2017)

(12) M. Lu, and Khai D. T. Ngo: "Comparison of Passive Shields for Coils in Inductive Power Transfer", Applied Power Electronics Conference and Exposition, pp. 1419-1424 (2017)

(13) Su Y. Choi, BeomW. Gu, Sung W. Lee, Woo Y. Lee, and J. Huh: "Generalized Active EMF Cancel Methods for Wireless Electric Vehicles", IEEE TRANSACTIONS ON POWER ELECTRONICS, Vol. 29, No. 11, pp. 5770-5783 (2014)

(14) S. Lee, W. Lee, J. Huh and C. Rim., "Active EMF cancellation method for I-type pickup of online electric vehicles," 2011 Twenty-Sixth Annual IEEE Applied Power Electronics Conference and Exposition (APEC), pp. 1980-1983 (2011)

(15) H. Cui, W. Zhong, H. Li, F. He, M. Chen and D. Xu: "A Study on the Shielding for Wireless Charging Systems of Electric Vehicles", Applied Power Electronics Conference and Exposition, pp. 1336-1343 (2018)

(16) S. Kim, H. Park, J. Kim, J. Kim, and S. Ahn: "Design and Analysis of a Resonant Reactive Shield for a Wireless Power Electric Vehicle", IEEE TRANSACTIONS ON MICROWAVE THEORY AND TECHNIQUES, Vol. 62, No. 4, pp. 1057-1066 (2014)

Keita Furukawa (Student member) received his B.S. and M.S. degrees in electrical, electronics and information engineering from Nagaoka University of Technology, Niigata, Japan in 2016 and 2018, respectively. He is currently a Ph.D. candidate at Nagaoka University of Technology, Niigata, Japan. His research interests include an inductive power transfer. He is a member of the Institute of Electrical Engineers of Japan and the Institute of Electrical and Electronics Engineers.

Keisuke Kusaka (Member) received the B.S. and M.S. degrees in electrical, electronics and information from Nagaoka University of Technology, Niigata, Japan in 2011, 2013, respectively. From 2015 to 2016, he was with Swiss Federal Institute of Technology in Lausanne (EPFL), Switzerland as a trainee. In 2016, he received the Ph.D. degree in energy and environment science from Nagaoka University of Technology. He was with Nagaoka University of Technology, Niigata, Japan as a researcher from 2016 to 2018. Since 2018, he has been with Nagaoka University of Technology, Niigata, Japan as an assistant professor. His current research interests include the areas of IPT systems and high-frequency converters. He is a member of Institute of Electrical Engineers of Japan, Society of Automotive Engineers of Japan and the IEEE.

Jun-ichi Itoh (Senior member) received his M.S. and Ph.D. degree in electrical and electronic systems engineering from Nagaoka University of Technology, Niigata, Japan in 1996, 2000, respectively. From 1996 to 2004, he was with Fuji Electric Corporate Research and Development Ltd., Tokyo, Japan. He was with Nagaoka University of Technology, Niigata, Japan as an associate professor. Since 2017, he has been a professor. His research interests are matrix converters, dc/dc converters, power factor correction techniques, energy storage system and adjustable speed drive systems. He received IEEJ Academic Promotion Award (IEEJ Technical Development Award) in 2007. In addition, he also received Isao Takahashi Power Electronics Award in IPEC-Sapporo 2010 from IEEJ, 58th OHM Technology Award from The Foundation for Electrical Science and Engineering, November, 2011, Intelligent Cosmos Award from Intelligent Cosmos Foundation for the Promotion of Science, May, 2012, and Third prize award from Energy Conversion Congress and Exposition-Asia, June, 2013. Prizes for Science and Technology (Development Category) from the Commendation for Science and Technology by the Minister of Education, Culture, Sports, Science and Technology, April 2017. He is a senior member of the Institute of Electrical Engineers of Japan, the Society of Automotive Engineers of Japan and the Institute of Electrical and Electronics Engineers.